Journal of Experimental Botany, Vol. 68, No. 5 pp. 1083–1095, 2017
doi:10.1093/jxb/erx023

RESEARCH PAPER

AtPME3, a ubiquitous cell wall pectin methylesterase of *Arabidopsis thaliana*, alters the metabolism of cruciferin seed storage proteins during post-germinative growth of seedlings

Stéphanie Guénin[1,2], Julie Hardouin[3], Florence Paynel[4], Kerstin Müller[5], Gaëlle Mongelard[2], Azeddine Driouich[4], Patrice Lerouge[4], Allison R. Kermode[5], Arnaud Lehner[4], Jean-Claude Mollet[4], Jérôme Pelloux[1], Laurent Gutierrez[2,*] and Alain Mareck[4,*,†]

[1] BIOPI Biologie des Plantes et Innovation EA3900, Université de Picardie Jules Verne, 33 Rue Saint Leu, 80039 Amiens Cedex, France
[2] CRRBM, Bâtiment Serres Transfert, Université de Picardie Jules Verne, 33 Rue Saint Leu, 80039 Amiens Cedex, France
[3] Université de Rouen Normandie, CNRS, Laboratoire PBS, 76000 Rouen, France
[4] Université de Rouen Normandie, Laboratoire Glyco-MEV, 76000 Rouen, France
[5] Department of Biological Sciences, Simon Fraser University, 8888 University Drive, Burnaby, BC V6A 1S6, Canada

* These authors contributed equally.
† Correspondence: alain.mareck@univ-rouen.fr

Received 9 September 2016; Editorial decision 10 January 2017; Accepted 11 January 2017

Editor: Gerhard Leubner, Royal Holloway, University of London

Abstract

AtPME3 (At3g14310) is a ubiquitous cell wall pectin methylesterase. *Atpme3-1* loss-of-function mutants exhibited distinct phenotypes from the wild type (WT), and were characterized by earlier germination and reduction of root hair production. These phenotypical traits were correlated with the accumulation of a 21.5-kDa protein in the different organs of 4-day-old *Atpme3-1* seedlings grown in the dark, as well as in 6-week-old mutant plants. Microarray analysis showed significant down-regulation of the genes encoding several pectin-degrading enzymes and enzymes involved in lipid and protein metabolism in the hypocotyl of 4-day-old dark grown mutant seedlings. Accordingly, there was a decrease in proteolytic activity of the mutant as compared with the WT. Among the genes specifying seed storage proteins, two encoding CRUCIFERINS were up-regulated. Additional analysis by RT-qPCR showed an overexpression of four *CRUCIFERIN* genes in the mutant *Atpme3-1*, in which precursors of the α- and β-subunits of CRUCIFERIN accumulated. Together, these results provide evidence for a link between AtPME3, present in the cell wall, and CRUCIFERIN metabolism that occurs in vacuoles.

Key words: Arabidopsis, AtPME3, CRUCIFERIN, etiolated hypocotyl, pectin methylesterase, seed germination, transcriptomic analyses.

Introduction

Seed germination requires a succession of interdependent events from imbibition to radicle protrusion. This period of intensive growth is accompanied by the biosynthesis of new cellular components and by the recycling of pre-formed storage components. In Arabidopsis, the presence of the seed endosperm cap constitutes the main constraint for radicle protrusion. Endosperm weakening and rupture are promoted by gibberellic acid (GA) and ethylene and inhibited by abscisic

Abbreviations:ABA, abscisic acid; DM, degree of methylation; HG, homogalacturonan; IEF, isoelectric focusing; PME, pectin methylesterase; WT, wild type.

acid (ABA) (Kucera *et al.*, 2005; Linkies *et al.*, 2009). These events are correlated with the induction of remodeling enzymes in the cell wall such as glycosyl hydrolases (Holdsworth *et al.*, 2008) and pectin methylesterases (PMEs) (Ren and Kermode, 2000, Scheler *et al.*, 2015). Moreover, GA induces an increase of total PME activity in germinating seeds (Ren and Kermode, 2000). During the germination process and early seedling growth, seeds mobilize their reserves such as starch, storage lipids and proteins (Bove *et al.*, 2001). For example, 11–12S globulins and 2S albumins are accumulated in vacuoles during seed maturation. These proteins are degraded during post-germinative growth to supply the young seedling with the first nutrient source prior to its transition to autotrophic growth (Bewley and Black, 1994; Gallardo *et al.*, 2001; Wan *et al.*, 2007). Numerous studies have highlighted change in gene expression and in protein and metabolite composition during seed germination and seedling development (Gallardo *et al.*, 2002; Zhao *et al.*, 2005; Fait *et al.*, 2006; Irshad *et al.*, 2008).

Development of the etiolated hypocotyl is well documented in Arabidopsis. Growth of this organ occurs exclusively by cell elongation in the dark (Gendreau *et al.*, 1997). Elongation requires an extensive synthesis and remodeling of cell wall components to effect an increased rigidity of the cell wall. Forty-eight hours after germination, the growth rate increases four- to five-fold with elongation starting from the lower part and propagating to the top of the hypocotyl (Refrégier *et al.*, 2004). During this fast growth, organ expansion is primarily a consequence of cell wall remodeling (Derbyshire *et al.*, 2007; Pelletier *et al.*, 2010).

Cell walls are mainly composed of interacting polysaccharides. Cell wall proteins contain multiple enzymatic activities for modifying the cell wall polysaccharides, as well as the structural glycoproteins and proteoglycans that participate in the wall organization. Polysaccharides are composed of three main polymers: cellulose, hemicelluloses and pectins. In the primary cell wall, cellulose is assembled into microfibrils coated with xyloglucans that interact with other cell wall components in a complex molecular network (Carpita and Gibeaut, 1993). Homogalacturonan (HG), the main pectin component, is synthesized in a highly methylated form prior to undergoing varying degrees of demethylation in the cell wall, a modification effected by PMEs (Goldberg *et al.*, 1986). Highly methylated HG is required at all stages of rapid cell expansion whereas weakly methylated HG appears when the cell growth ceases (Pelletier *et al.*, 2010; Wolf *et al.*, 2012). In the presence of calcium, the demethylated HG is more susceptible to forming 'egg-box' structures (i.e. interaction of negatively charged HGs via calcium bridges), thus strengthening the cell wall.

The model in which a reduction of DM of HG is connected to growth arrest is likely more complex. Indeed, rapid cell elongation has been shown to be correlated with a high DM of pectins reaching a minimum of 60% in 3-day-old Arabidopsis hypocotyls (Derbyshire *et al.*, 2007). However, upon GA treatment, the elongation of Arabidopsis hypocotyls still increases but no changes of the DM of HG are observed (Derbyshire *et al.*, 2007). Intriguingly, etiolated Arabidopsis hypocotyls require pectin demethylation in the wall 48 h after imbibition to move from the slow to the fast growth rates (Pelletier *et al.*, 2010). In this case, the decrease of pectin DM would render pectin polymers more susceptible to pectin-degrading enzymes such as polygalacturonases (PGases) for the remodeling of the cell wall, pectin turnover and/or growth (Willats *et al.*, 2001; Pelletier *et al.*, 2010).

A previous proteomic study showed that cell wall modifying enzymes were abundant during hypocotyl elongation, particularly during active growth (Irshad *et al.*, 2008). Five PME isoforms, including AtPME3 (At3g14310), and two PGase isoforms were notably detected during the active growth phase. These proteins associated with pectate lyases (PLs) could be involved in the pectin cleavage and/or turnover that occur during the cell wall remodeling process (Sénéchal *et al.*, 2014). Proteolytic activities were globally also promoted during the active growth stage for possible maturation and/or degradation of proteins (Irshad *et al.*, 2008). Finally, proteins involved in lipid metabolism were also abundant in the wall during the stage of hypocotyl active growth (Irshad *et al.*, 2008).

As mentioned previously, the transition from the slow to the fast elongation rate in hypocotyls is accompanied by a decrease of the DM of HG. Consequently, AtPME3, physically present in hypocotyl cell walls (Irshad *et al.*, 2008; Guénin *et al.*, 2011), is a possible partner in association with other enzymes for acting on HG. Interestingly, AtPME3 activity is optimal *in vitro* on HG with a DM of about 90% (Guénin *et al.*, 2011; Sénéchal *et al.*, 2015). This PME isoform is ubiquitously expressed in Arabidopsis seedlings and in adult plants (Zhao *et al.*, 2005). Moreover, the *AtPME3* promoter is particularly active in leaves, stems, and roots of seedlings (Guénin *et al.*, 2011). Distinct roles were attributed to this PME such as an effect on adventitious rooting and on plant–nematode interactions (Hewezi *et al.*, 2008; Guénin *et al.*, 2011). Such roles may also depend on the PME regulation by a specific PME inhibitor (PMEI) (Jolie *et al.*, 2010). Analysis of previous transcriptomic data highlighted the correlation of gene expression of PME and PMEI in different tissues and at all developmental stages in Arabidopsis (Wolf *et al.*, 2009).

To address the functions of the ubiquitous AtPME3 in seedling development, we performed a transcriptomic analysis on 4-day-old etiolated hypocotyls from the *Atpme3-1* loss-of-function mutant (Guénin *et al.*, 2011) comparing it with that found in hypocotyls of equivalently treated wild type (WT) seedling. At the phenotypic level, the mutant seeds germinated earlier and the seedlings displayed less root hairs than the WT. Most significantly and surprisingly, several vacuolar storage proteins including CRUCIFERINS accumulated in the mutant, suggesting a link between the cell wall PME3 and CRUCIFERIN metabolism.

Materials and methods

Plant materials and growth conditions

Four-day-old etiolated seedlings derived from seeds of the wild type (WT) and mutant (*Atpme3-1*) of *Arabidopsis thaliana* (ecotype Columbia) were grown as described in Pelletier *et al.* (2010). The *Atpme3-1* mutant was previously characterized by Guénin *et al.* (2011). Six-week-old plants were harvested after growth on sterilized

soil in a chamber with a 16 h photoperiod at 200 µmol photon m^{-2} s^{-1} with a day/night temperature cycle of 20 °C/16 °C and daily watering.

Seed germination

Seeds were harvested at maturity and stored in the dry state for 4–8 weeks at 4 °C. Seeds were sterilized with 70% (v/v) ethanol. Fifty seeds were transferred onto the germination medium composed of half-strength Murashige and Skoog medium (Sigma-Aldrich), pH 6.2, solidified with 1% (w/v) agar in Petri dishes. Seeds were stratified at 4 °C for 2 d in the dark then transferred to a growth chamber at 24 °C with a 16-h light photoperiod and 120 µE m^{-2} s^{-1} intensity. Seed germination (i.e. seeds with endosperm rupture and emerged radicles) was then counted daily for 7 d. Endosperm rupture was scored under a dissecting microscope. Four plates were used for each replicate. Where indicated, 1 µM ABA was added to the germination medium.

Characterization of seed and seedling phenotypes

Phenotypic characterization of at least 40 four-day-old etiolated seedlings from WT and *Atpme3-1* was performed using 50-fold enlarged photographs acquired with a stereomicroscope (MZ FLIII; Leica). Root and shoot length, and root hair number and length were measured with ImageJ (Abramoff *et al.*, 2004).

Analyses of seed mucilage were performed after seed imbibition in water for 3 h. Mucilage released from WT and *Atpme3-1* seeds was stained for 30 min with 0.02% (w/v) ruthenium red and washed with water before observation with a stereomicroscope (MZ FLIII; Leica).

Protein extraction and quantification

Six-week-old plants or separated organs of 4-day-old etiolated seedlings were ground in 20 mM sodium phosphate buffer, pH 7.5, 1 M NaCl, 0.2% (w/v) polyvinylpolypyrrolidone, 0.01% (w/v) Tween 20, one protease inhibitor cocktail tablet (Roche) for 3 h at 4 °C. Cellular fragments were discarded after centrifugation at 105 000 *g* for 30 min. Protein extracts were concentrated using Amicon PM10 membranes (Millipore) in water or in 20 mM sodium phosphate buffer, pH 7.5. Proteins were quantified using the Bradford microassay (Bradford, 1976), with the Bio-Rad kit and bovine serum albumin as a standard.

Enzymatic assays

PME samples were incubated for 15 min at 25 °C in 100 mM sodium phosphate, pH 7.5 with 1% (w/v) citrus pectins (82% DM, Sigma). Methanol produced by catalysis was then quantified using the alcohol oxidase method (Klavons and Bennett, 1986); 1 IU of PME activity generates the liberation of 1 µmol of methanol min^{-1}. Activity values were calculated from three to eight independent replicates prior to zymography.

Protease activity

Protease activity was evaluated with casein as a substrate using the method described by Cupp-Enyard (2008). Experiments were carried out twice with 0.5 mg and twice with 1 mg of proteins extracted from 6-week-old WT and *Atpme3-1* plants. Standard curves were obtained with tyrosine ranging from 0.055 to 0.553 µmoles. Data were expressed in nanomoles of released tyrosine per minute per milligram of proteins.

Isoelectric focusing and zymogram analysis

Isoelectric focusing (IEF) was performed on ultrathin polyacrylamide slab gels (0.3 mm) with 3.5–10.0 pH range (Pharmalytes) in 5% acrylamide according to the manufacturer's procedure with a Multiphor II system (LKB-Pharmacia). Samples containing from 0.05 to 0.1 UE of PME activity (Klavons and Bennett, 1986) were loaded at the anode side. After IEF, gels were washed for 30 min in 20 mM Tris–HCl pH 8.5, 5 mM EDTA. PME activity was monitored in gel (zymography) by using a sandwich of 1% (w/v) citrus pectin (82% DM, Sigma-Aldrich)–1% (w/v) agar according to Bertheau *et al.* (1984). Sandwiches were incubated for 1 h at 25 °C. Demethylated pectins by PME activities were precipitated with 0.1 M malic acid and stained by 0.02% (w/v) ruthenium red.

SDS-PAGE and western blot analyses

SDS-PAGE was performed on 12% (w/v) acrylamide gels according to Laemmli (1970), using a slab gel system (Mini Protean II, Bio-Rad). Proteins were stained with Coomassie blue or silver. After SDS-PAGE, western blots were carried out on a 0.2 µm polyvinylidene fluoride membrane (Bio-Rad) according to Towbin *et al.* (1979). Blots were treated for 2 h with *Brassica napus* anti-cruciferin polyclonal antibodies (dilution 1/5000) (Wan *et al.*, 2007) before being detected by electroluminescence with horseradish peroxidase (Pierce ECL). Polyclonal antibodies directed against CRUCIFERINS were a generous gift of Dr D. D. Hegedus (Saskatoon, Canada).

Nano liquid chromatography–tandem mass spectrometry analyses

Protein bands excised from gels were treated with trypsin (Promega) (Shevchenko *et al.*, 1996). Peptides were analysed with an LTQ-Orbitrap Elite coupled to an Easy nLC II system (both from Thermo Scientific) according to Ouidir *et al.* (2015). After injection into an enrichment column (C18 PepMap100, Thermo Scientific), sample separation was performed with an analytical column needle (NTCC-360/100-5-153, NikkyoTechnos). The mobile phase consisted of H_2O–formic acid 0.1% and acetonitrile–formic acid 0.1% (buffer A). Tryptic peptides were eluted at a flow of 300 nl min^{-1}, from 2% to 40% buffer A in 45 min. The mass spectrometer was operated in positive ionization mode, with capillary voltage and source temperature set at 1.5 kV and 275 °C. Multi-charged peptides were analysed by collision-induced dissociation (Top 20) in the mass range *m/z* 400–1800.

Raw data files were processed using Proteome Discoverer 1.3 software (Thermo Scientific). Peak lists were searched using the MASCOT search engine (Matrix Science) against the *Arabidopsis thaliana* database with the following conditions: missed cleavage sites allowed; variable modifications: carbamidomethylation of cysteine and oxidation of methionine. Parent ion and daughter ion tolerances were 10 ppm and 0.5 Da. Proteins were considered identified if at least two peptides were identified with a score above 20.

RNA isolation and cDNA synthesis

Dry seeds or 24-, 48- and 96-h dark grown seedlings from WT and *Atpme3-1* mutant were frozen and ground in liquid nitrogen for three independent biological replicates. Total RNA was extracted as described by Gutierrez *et al.* (2006) and treated with DNase I using a DNA *free* Kit (Ambion). cDNA was synthesized by reverse transcribing 4 µg of RNA using the Transcriptor High Fidelity cDNA synthesis kit (Roche) according to the manufacturer's instructions.

Real-time RT-qPCR

CRUCIFERIN transcript levels were assessed in three independent biological replicates by real-time RT-qPCR in assays with duplicate reaction mixtures containing 0.5 µM of primers, 5 µl of cDNA, 1× HOT FirePol® Evagreen® qPCR Mix Plus (Capillary) (Solis Biodyne) with the Light Cycler 1.5 instrument (Roche Diagnostics, Germany). Primers (5′ and 3′) were for CRU4: GACAGCTCATAGCCGT and CTTGCTTCTTCGGGTG; for CRB: AACGAAAACG CACAGGTCAA and GCTATGGGTCAGTCAGTGTGGTCT;

for CRC: AACATGAACGAACGCTAACGAG and TGTTTCCGT GGGACTG; and for CRD: TACATTAACACACTGAGCGGC and AGAAGAGCTTGGTGTCATAGAC. Standard amplification protocol and data analysis were carried out as in Gutierrez *et al.* (2008), using GeNorm validated (Vandesompele *et al.*, 2002) *CLATHRIN* and *PEX4* reference genes. Fig. 3 shows normalized expression patterns obtained using *PEX4* as reference; data obtained using *CLATHRIN*, displaying similar expression levels, are shown in Supplementary Fig. S1 at *JXB* online. A Kruskall–Wallis test combined with a Shapiro–Wilk test was performed to analyse the differences between the germination/growth stages.

Microarray analysis

Six independent batches of 300 WT and 300 mutant hypocotyls were prepared. Hypocotyls collected from dark-grown seedlings (96 h after germination) were frozen and ground in liquid nitrogen. RNA extraction was performed following a hot phenol purification protocol (Verwoerd *et al.*, 1989; Gutierrez *et al.*, 2006). RNA quality was assessed using Bio-Rad Experion with the Eukaryote Total RNA StdSens kit. Double stranded cDNAs were synthesized from 20 µg total RNA according to the 'cDNA synthesis system' from Roche. Samples were Cy3 labeled using NimbleGen One-Color DNA labeling kit and loaded on a NimbleGen Arabidopsis 12 × 135K array. Samples were hybridized for 19 h at 42 °C on a NimbleGen hybridization system. After washing with the NimbleGen Wash Buffer Kit, slides were scanned at 2.5 µm pixel resolution using the Axon GenePix 4400 A scanner (Molecular Devices, LLC, Sunnyvale, CA, USA) piloted by GenePix Pro 7 software (Molecular Devices). Scanned images (TIFF format) were imported into Nimblescan software (NimbleGen Systems, Inc., Madison, WI, USA) for metrics parameter control. Pair files were then generated. Subsequent analyses were performed using the ANAIS (Analysis of NimbleGen Arrays Interface) web interface (Simon and Biot, 2010). Data were normalized using the robust multiarray averaging (RMA) normalization method. Results are the mean of six independent biological replicates.

Gene and protein annotations

Gene and protein annotations were obtained from accessible databases. Protein characteristics were extracted from UniProtKB/Swiss-Pro. The gene expression in the WT was collected from AraNet/PlaNet. Subcellular localization of proteins was predicted with WoLF PSORT (Horton *et al.*, 2007).

Co-expression network of genes in the Atpme3-1 *mutant obtained from the transcriptomic data*

The network of gene co-expression was constituted with genes obtained from the transcriptomic data plus *AtPME3* with the GeneMANIA server (Toronto University, Canada; Warde-Farley *et al.*, 2010). Genes showing a significant variation in their expression levels ($-2 \geq \log_2$ *Atpme3-1*/WT≥ 2) (464 loci) were submitted for network building. Ninety-five genes were highly connected with *AtPME3* in the resulting network of co-expression characterizing the *Atpme3-1* mutant.

Statistical analysis

Data were analysed by ANOVA ($P<0.05$) for statistical significance using QuickCalc (GraphPad Inc.) or Statistica (StatSoft Inc.), or with the Kruskal–Wallis comparison *post hoc* test.

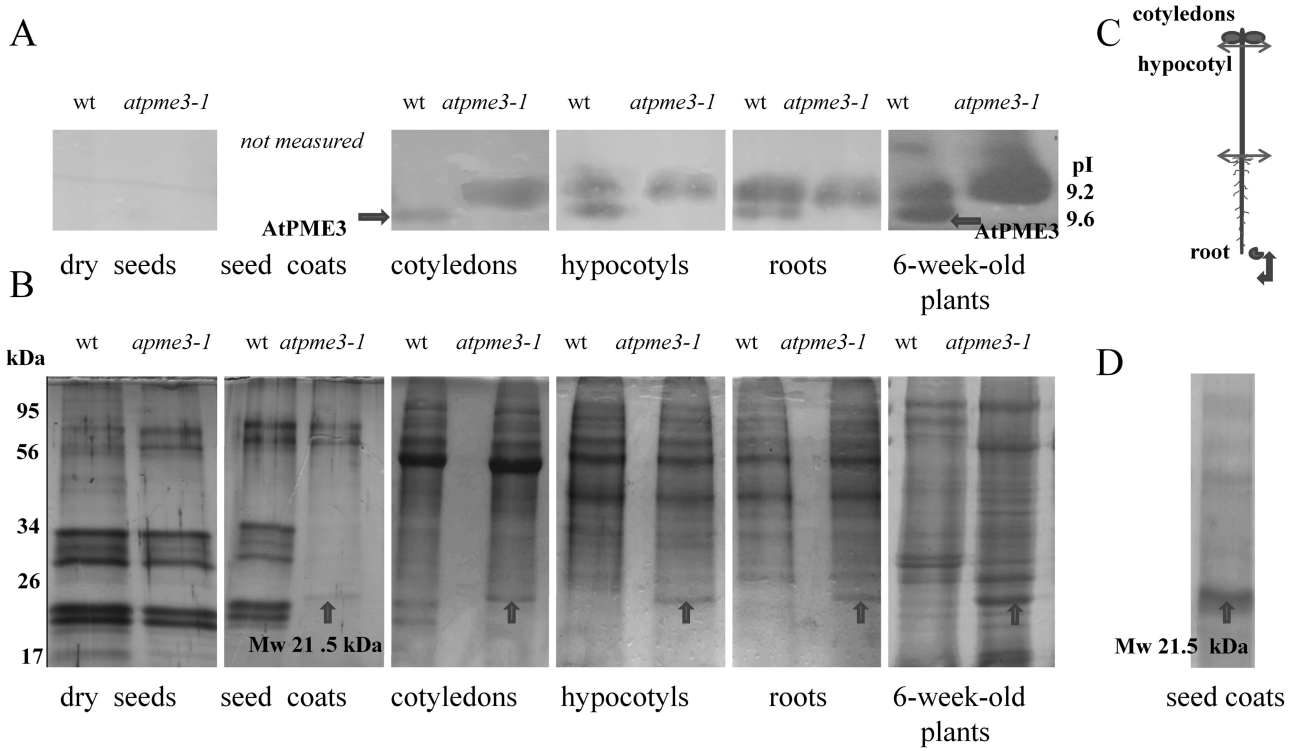

Fig. 1. Comparative protein profiles and PME activities of WT and *Atpme3-1*. Analyses were performed on dry seeds, 4-day-old dark-grown seedlings and 6-week-old plants. (A) Zymogram showing activity of PME protein bands on an IEF gel, which were revealed by incubation with ~0.05 IU of PMEs for assays on the different seedling organs and ~0.1 IU of PMEs for assays on 6-week-old plants. (B) Protein profiles. Proteins (40 µg) were separated by SDS-PAGE and stained with Coomassie blue. (C) Drawing showing the different organs used for analyses of seedlings: cotyledons with the apical meristem, hypocotyl and roots. (D) Electrophoresis gel for A*tpme3-1* seed coat extract stained with the silver reagent. AtPME3 activity spot in (A) and 21.5 kDa protein in (B) are indicated with arrows.

AQ1

Results

A PME isoform with a pI 9.6 is lacking in all organs of the Atpme3-1 *mutant*

The PME activity zymography was performed in seeds, seedling organs (as defined in Fig. 1C), and 6-week-old plants from WT and *Atpme3-1* (Fig. 1A). In wild type, the activity of two basic spots migrating at pI 9.2 and 9.6 was detected in seedling hypocotyls and roots as well as in 6-week-old plants. In *Atpme3-1* only the isoform at pI 9.2 was detected, indicating that the band at pI 9.6 was likely to be due to PME3 activity, as previously suggested (Guénin *et al.*, 2011). Interestingly, in WT cotyledons, PME activity seemed to be only due to AtPME3; only the spot at pI 9.6 was visible on the isoelectric focalization gel (IEF) tracks. In addition, loss of AtPME3 activity in the mutant cotyledon triggered the expression of the other PME isoform migrating at pI 9.2. In *Atpme3-1* and WT seeds, PME activity was below the detection limit.

A protein of 21.5 kDa is accumulated in the Atpme3-1 *mutant*

Dry seeds of WT and *Atpme3-1* displayed similar protein profiles (Fig. 1B) with two subsets of proteins at ~20 and 30 kDa, likely representing the α- and β-subunits of the 11–12S globulin (CRUCIFERIN)—the most abundant storage proteins of Arabidopsis seeds (Shimada *et al.*, 2003). In contrast, the protein content in seed coats released from 4-day-old etiolated seedlings was different between WT and the mutant (Fig. 1B). The profile of WT seed coat proteins was similar to the one observed in WT dry seeds. To the contrary, seed coats of *Atpme3-1* displayed a protein profile that lacked the two protein subsets, but possessed a protein of 21.5 kDa (Fig. 1B, D). A protein at 21.5 kDa similarly accumulated in all seedling organs and was particularly visible in 6-week-old *Atpme3-1* plants (arrows in Fig. 1B). This band was not detectable in WT.

Transcriptomic analysis of 4-day-old etiolated seedling hypocotyls revealed several down-regulated genes in Atpme3-1 *compared with wild type*

To evaluate the possible transcriptional modulations triggered by *AtPME3* knock-out and determine which genes encode the 21.5 kDa protein that accumulated in the mutant, a microarray analysis was performed on hypocotyls of 4-day-old dark-grown seedlings from *Atpme3-1* and WT. The complete dataset can be found on GEO under the accession number GSE75326. Expression levels of 464 genes displayed significant variation in *Atpme3* compared with WT ($-2 \leq \log_2$ *Atpme3-1*/WT≤ 2), consisting of 324 down-regulated genes and 140 up-regulated genes.

The distribution of the differentially expressed genes in *Atpme3-1* is shown in Fig. 2A based on their putative involvement in biological processes. The largest group encoded proteins involved in developmental processes (78 genes described in Supplementary Table S1). The second largest group encoded proteins related to transport and homeostasis, in which 28 genes were down-regulated (Fig. 2A).

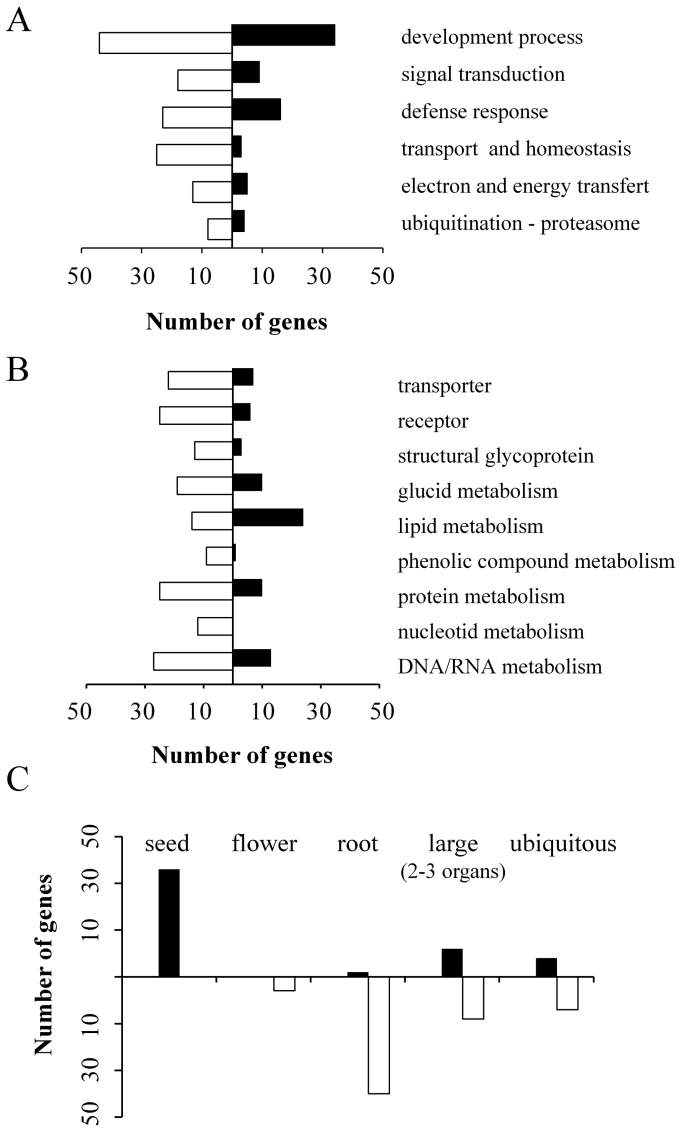

Fig. 2. Analyses of microarray data showing up-regulated (black) and down-regulated (white) genes in *Atpme3-1* compared with WT. Only the genes with strong modification in their expression were considered (–2≥log2 *Atpme3-1*/WT≥2): 166 down-regulated genes and 74 up-regulated genes. (A) Distribution of the differentially expressed genes according to their putative roles in different biological processes. (B) Distribution of the differentially expressed genes according to the putative biochemical function. (C) Organ specificity was predicted for 70 genes differentially expressed in *Atpme3-1* that encoded proteins involved in development. Prediction was assessed with the AraNet database (PlaNet). When genes were expressed in two or three different organs, they were considered as large. When genes were expressed in all organs they were labelled as ubiquitous.

Differentially expressed genes in *Atpme3-1* were also classified according to their putative biochemical functions (Fig. 2B). Most of the down-regulated genes (white bars) encoded transporters and receptors or proteins involved in protein and DNA/RNA metabolism (Fig. 2B). Nine of them encoded putative transporters specific for heavy metals such as *ZIP8* and *ZIP9* specialized in zinc transport (Mäser *et al.*, 2001).

The organ-specific expression of the 70 differentially expressed genes putatively involved in developmental processes was predicted by *in silico* analysis with the AraNet database (Fig. 2C). Most of the up-regulated genes in *Atpme3-1* were predicted to be mainly expressed in seeds. Interestingly, among them, *MEE8* (*MATERNAL EFFECT EMBRYO ENDING8*), encoding a transcription factor involved in seed dormancy termination, was found to be 3.4-fold more highly expressed in *Atpme3-1* as compared with the WT (Supplementary Table S1). Most of down-regulated genes were predicted to be expressed in roots (Fig. 2C) with 18 genes that encode proteins putatively involved in root hair differentiation or development (Supplementary Table S1).

Genes encoding proteins putatively involved in cell wall organization and remodeling are mainly down-regulated in hypocotyls of the Atpme3-1 *mutant*

The expression of genes related to cell wall modification was mainly down-regulated in *Atpme3-1* (Supplementary Table S2). Among the genes encoding structural glycoproteins involved in cell wall organization, 12 were down-regulated in the mutant and only four of them were up-regulated. Moreover, six genes encoding peroxidases, possibly implicated in lignin biosynthesis and extensin cross-linking, were down-regulated. Interestingly, two genes (*WAKL5* and *WAKL8*) (*Wall Associated receptor-like Kinase*) (Steinwand and Kieber, 2010), were also down-regulated. In conclusion, the expression of a set of genes encoding proteins involved in specifying the structure of the cell wall, cell wall remodeling, or signaling in the cell wall, is affected in *Atpme3-1*.

Eight genes encoding proteins that were directly linked to pectin metabolism were down-regulated in *Atpme3-1* (Table 1): three *PMEs* (*PME11*, *PME24* and *PME46*), one PGase (*ADPG1*) and four *PECTATE LYASES*. The loss of *PME3* expression was not compensated by up-regulation of any of the 65 other putative *PMEs*. This result is in agreement with the PME activity observed by zymogram analyses in *Atpme3-1* seedling hypocotyls, a possible compensatory activity spot being detected only in *Atpme3-1* cotyledons (Fig. 1A). In addition, no change in the expression of *PMEI* genes was detected in *Atpme3-1*.

Changes in the expression of genes involved in lipid and protein metabolism

Among the differentially regulated genes encoding proteins involved in lipid metabolism (Supplementary Table S3), eight were down-regulated and nine were up-regulated in *Atpme3-1* hypocotyls. Interestingly, 14 genes encoding proteins involved in the biosynthesis of seed lipid (triglyceride) reserves and oil body proteins (e.g. oleosins *OLE2* and *OLE3*) during seed maturation were differentially expressed (12 were up-regulated and two were down-regulated in *Atpme3-1* hypocotyls).

The common 21.5-kDa protein accumulated in all organs and at every stage of *Atpme3-1* development (Fig. 1B, D) was of interest (see subsequent discussion). A list of 35 genes related to protein metabolism was established by comparing the transcriptomes of the hypocotyls from *Atpme3-1* and WT (Supplementary Table S4). Most of the differentially expressed genes (71%) were down-regulated; notably ten were genes involved in protein phosphorylation/dephosphorylation: nine have a predicted kinase activity and one a predicted phosphatase activity. Among them, *At1g16260* encodes a Wall Associated Kinase-Like: WAKL8. Ubiquitination and the proteasome pathway were represented by 13 genes, with eight of them exhibiting down-regulation in the mutant. This may suggest a modification in the protein turnover in the mutant hypocotyl via selective proteasome-mediated protein degradation. Moreover, six down-regulated genes encoded proteases: one is predicted to be localized in the cytoplasm (At3g48340), and the five others in the cell wall (Table 2). Two wall protease inhibitor genes were found to be either up-regulated (*At1g47450*) or down-regulated (*At2g25240*). In addition, four genes exhibiting a modified expression in *Atpme3-1* hypocotyls were related to protein storage function. The two up-regulated genes encode CRUCIFERINS (typically specific to seeds), while the two down-regulated genes code for GERMIN-LIKE proteins that are normally expressed in roots (Ham *et al.*, 2012). Thus, we focused on *CRUCIFERIN* expression and protein composition.

Three unprocessed CRUCIFERINS and their α- and β-subunits accumulated in Atpme3-1

A significant up-regulation of the expression of genes encoding CRUCIFERINS, *CRB* and *CRD*, was detected in the *Atpme3-1* microarray studies (Table 2). These proteins were interesting because they were likely to be those that could not

Table 1. *List of genes extracted from transcriptomic data specifying proteins involved in pectin remodeling*

Locus	Gene symbol	Annotation	Catalytic activity	Pectin process	$\log_2$ *Atpme3-1 vs* WT	*P*-value
AT2G21610	*PME11*	Pectin methylesterase 11	Methyl esterase	Regulation of ionic charge	–2.413	0.005
AT3G10710	*PME24*	Pectin methylesterase 24	Methyl esterase	Regulation of ionic charge	–3.449	0.346
AT5G04960	*PME46*	Pectin methylesterase 46	Methyl esterase	Regulation of ionic charge	–3.656	0.762
AT3G57510	*ADPG1*	Polygalacturonase ADPG1	Hydrolase	Pectin degradation	–2.453	0.191
AT1G05650	*F3F20.10*	Pectin lyase like protein	Lyase	Pectin degradation	–2.998	1.201
AT1G05660	*F3F20.11*	Pectin lyase like protein	Lyase	Pectin degradation	–2.724	0.887
AT4G22080	*RHS14*	Probable pectate lyase 16	Lyase	Pectin degradation	–2.467	0.241
AT4G22090	*F1N20.190*	Putative pectate lyase 17	Lyase	Pectin degradation	–2.087	0.07

Table 2. *List of genes implicated in protein metabolism*

The list shows five down-regulated genes encoding proteases, two for protease inhibitors and two for storage proteins normally involved in the nutrient reservoir activity in seed vacuoles.

Locus	Gene symbol	Annotation	Catalytic activity	Biological process/molecular function	Cell localization	log_2 *Atpme3-1 vs* WT	*P*-value
Proteolytic activity							
AT1g43780	*SCPL44*	Serine carboxypeptidase-like 44	Protease	Protein metabolism	Cell wall	–2.772	0.2.91
AT1G61130	*SCPL32*	Serine carboxypeptidase-like 32	Protease	Protein metabolism	Cell wall	–3.11	0.333
AT1G79320	*MC6*	Metacaspase 6	Endopeptidase	Defense response	Cytoplasm	–2.424	0.171
AT3G48340	*CEP2*	Cys endopeptidase 2	Protease	Programmed cell death	Endoplasmic reticulum	–2.746	0.606
AT3G51360		Aspartyl protease-like	Protease	Protein metabolism	Cell wall	–2.175	0.205
Inhibition of proteolytic activity							
AT1G47540		Defensive-like protein 192	Trypsin inhibitor-like	Defense response	Cell wall	2.58	0.131
AT2G25240	*CCP3*	Serpin-Z10	Protease inhibitor	Proteolysis regulation	Cell wall	–2.143	0.051
Storage activity							
AT1G03880	*CRB*	Cruciferin B		Nutrient reservoir activity	Seed—vascular leaf	2.116	0.154
AT1G03890	*CRD*	Rmlc-like cupin		Nutrient reservoir activity	Seed—vascular leaf	2.879	0.184
AT1G18970	*GLP4*	Germin-like protein 4	Manganese ion binding	Nutrient reservoir activity	Root	–2.536	0.488
AT4G14630	*GLP9*	Germin-like protein 9	Oxidoreductase	Nutrient reservoir activity	Root—senescing leaf	–2.691	0.123

be found in *Atpme3-1* seed coat (subsets at ~20 and ~30 kDa in Fig. 1B). In contrast, a 21.5 kDa protein accumulated in the mutant early during development and remained present at all stages. This protein could not be detected in the WT at any developmental stage.

In order to gain more insight into the expression regulation of *CRUCIFERIN* genes in the mutant, the expression of *CRU4*, *CRB*, *CRC* and *CRD* was quantified by RT-qPCR in dry seeds and in 1-, 2- and 4-day-old dark-grown seedlings from *Atpme3-1* and wild type (Fig. 3). In dry seeds, no significant difference was observed between mutant and wild type (i.e. the calibrator for which gene expression was set to 1) for the four genes. In seedlings, *CRB*, *CRC*, *CRD* showed similar expression variations. In all early developmental stages, these genes were expressed ~6–20 times more in the mutant compared with the WT. In contrast, *CRU4* expression in 1- and 2-day-old seedlings was only 2–6-fold higher in the mutant than in the WT. Nevertheless, in 4-day-old seedlings, *CRU4* was 20 times more expressed in the mutant.

CRUCIFERINS are synthesized as precursors with a molecular mass ranging from 45 to 55 kDa; they are then proteolytically cleaved to generate two subunits, the α- and β-subunit polypeptides (molecular masses of 27–35 and 20–22 kDa, respectively) each of which is linked by a disulfide bridge (Gruis *et al.*, 2004; Wan *et al.*, 2007). This processing is followed by the formation of a hexameric complex within protein storage vacuoles. In order to assess whether overexpression of *CRUCIFERIN* genes led to protein accumulation in *Atpme3-1* plants, proteins from 6-week-old mutant plants were analysed. The accumulation of three bands at 54, 35 and 21.5 kDa was characterized by SDS-PAGE after Coomassie blue staining of *Atpme3-1* extract (Fig. 4A). After blotting, anti-*Brassica napus* cruciferin antibodies allowed the detection of two bands in the mutant extract (Fig. 4B). These antibodies were previously shown to recognize unprocessed and α-subunit CRUCIFERIN forms (Wan *et al.*, 2007). These two protein bands, only very faintly recognized by the antibodies in the WT extract, were approximately at 54 and 35 kDa, in agreement with the molecular mass ranges of the unprocessed and α-subunit CRUCIFERIN. To further characterize the three accumulated proteins, analyses by nano liquid chromatography–tandem mass spectrometry (LC-MS/MS) were performed on bands excised from the gel (Fig. 4A). Three CRUCIFERIN were identified: CRB/At1g03880, CRC/At4g28520 and CRU4/At5g44120 in each of the 54, 35 and 21.5 kDa protein bands (Fig. 4C). The protein band at 54 kDa contained peptides distributed in the whole unprocessed sequence (amino acids in bold). Peptides found in the 35 kDa band were only localized in the α-subunit sequence (amino acid in italic) and those from the 21.5 kDa band in the β-subunit sequence (underlined amino acids). Peptides sequenced from CRC (At4g28520) provided the best coverage of the protein sequence: 40% for the unprocessed form, 68% for the α-subunit, and 81% for the β-subunit (Supplementary Table S5). Taken together, these findings suggest that CRUCIFERIN metabolism is enhanced in *Atpme3-1*.

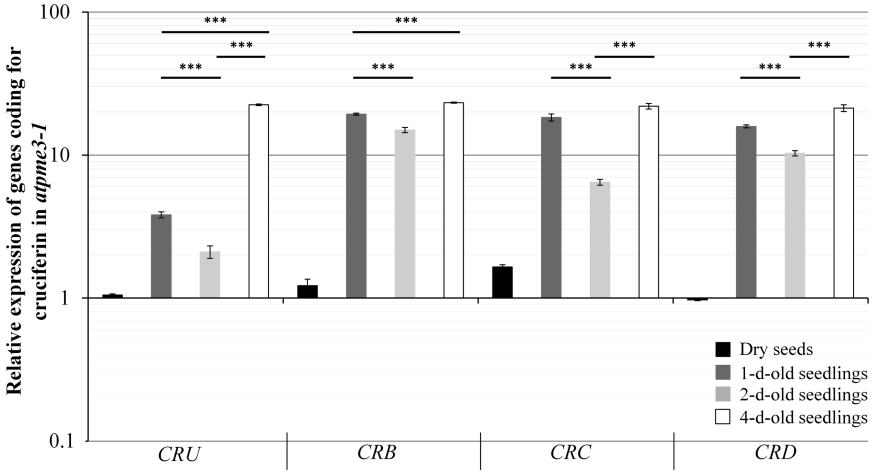

Fig. 3. RT-qPCR analyses of the expression of four *CRUCIFERIN* genes in *Atpme3-1* dry seeds and in 1-, 2- and 4-day-old seedlings grown in the dark. Gene expression was normalized using the validated reference gene *PEX4*. Error bars indicate ±SE obtained from technical duplicates from one biological replicate. The analysis was performed with two additional biological replicates and gave similar results. ***P<0.001 with the Kruskal–Wallis comparison *post hoc* test.

Proteolytic activity is decreased in Atpme3-1 *as compared with the wild type*

To assess whether proteolytic activity was affected in *Atpme3-1* plants, intracellular and cell wall proteins were extracted from 6-week-old Arabidopsis plants. As shown in Table 3, proteolytic activity was significantly lower in total extracts obtained from *Atpme3-1* compared with WT plants. Activity was reduced by approximately 40% in the cell compartment and by 55% in the cell wall protein extract from *Atpme3-1*.

Germination and root hair density are affected in Atpme3-1

In order to analyse the potential effect of CRUCIFERIN metabolism alteration on seedling development, we analysed seed germination. Seed germination was earlier in *Atpme3-1* compared with WT. Almost 10% of *Atpme3-1* seeds had germinated 24 h after imbibition. Maximum germination rate (98%) was reached 48 h after imbibition (Fig. 5A). In contrast, for WT seeds, no germination was observed 24 h after imbibition. The maximum germination rate was reached after 72 h. In the presence of 1 µM ABA, the endosperm rupture was still earlier in *Atpme3-1* seeds compared with WT (Fig. 5B).

In addition, the released mucilage was not affected in the mutant. As previously described for other ecotypes (Western *et al.*, 2001), seed mucilage of both WT and *Atpme3-1* showed two distinct layers: an inner one, intensively stained with ruthenium red, and an outer one, weakly colored with a similar aspect (Fig. 5C).

In a previous study, it was shown that *Atpme3-1* seedlings displayed no specific phenotype except an increased adventitious rooting (Guénin *et al.*, 2011). Root hair production is a quantitative trait that was not investigated before and our microarray analysis highlighted several down-regulated genes found in *Atpme3-1* that are putatively involved in root hair differentiation (Supplementary Table S1). Focusing on this developmental process, we observed that, while the mean of root hair length remained the same, root-hair density was significantly lower (−27%) in dark-grown *Atpme3-1* seedlings as compared with dark-grown WT seedlings (Supplementary Fig. S2).

Co-expression network of up- and down-regulated genes in the mutant

GeneMANIA (Warde-Farley *et al.*, 2010) was used to build a network (Fig. 6) with our transcriptomic data (Supplementary Table S6), linking the co-regulated genes, including *AtPME3*, which displayed significant expression modulation ($-2 \geq \log_2$ *Atpme3-1*/WT≥ 2). Ninety-six genes were highly connected, with 90.5% of co-expression. The network was mainly composed of two interconnected groups exhibiting distinct functions. The group in the lower part of Fig. 6 is directly linked to *AtPME3* and contains mostly genes involved in cell wall remodeling and root hair development, among which three genes encoded PMEs: *PME11*, *PME24* and *PME46*. Several genes in grey, normally co-expressed with those in black, have been included although their transcript levels remained stable. The upper part of the network contains genes mainly involved in storage lipid reserve accumulation/oil body biogenesis (OLEO2 and OLEO4, for example) or proteins (*At1g03880*/*CRB* and *At1g03890*/*CRD*, for example). Genes that belong to this part of the network are all up-regulated. Genes related to GA, ABA, the ubiquitination pathway and cell wall sensors (*MARIS*, *WAKL5* and *WAKL8*) are indicated by arrows.

Discussion

In Arabidopsis, AtPME3 was previously shown to be involved in adventitious rooting (Guénin *et al.*, 2011), in root hypersensitivity to zinc (Weber *et al.*, 2013) and in nematode infection (Hewezi *et al.*, 2008). This diversity of biological functions played by AtPME3 is probably the consequence

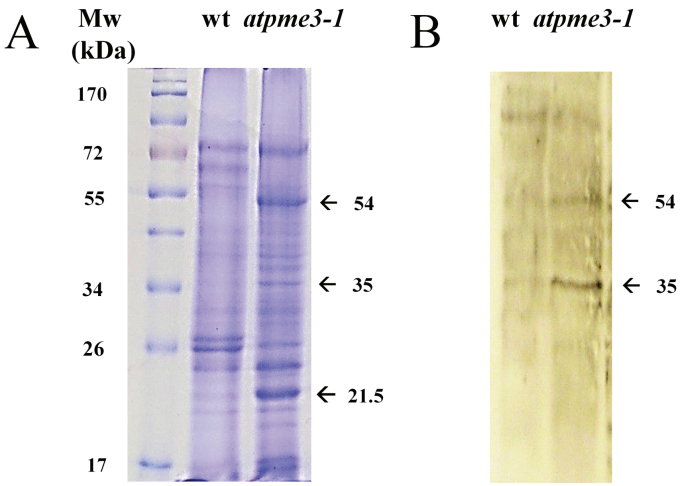

C

CRB

MGRVSSIISF SLTLLILFNG YTAQQWPNEC QLDQLNALEP SQIIKSEGGR
IEVWDHHAPQ ***LR***CSGFAFER ***FVIEPQGLFL*** ***PTFLNAGK***LT FVVHGRGLMG
RVIPGCAETF MESPVFGEGQ GQGQSQGFRD MHQKVEHLRC GDTIATPSGV
AQWFYNNGNE PLILVAAADL ASNQNQLDRN LRPFLIAGNN PQGQEWLQGR
KQQKQNNIFN GFAPEILAQA FK***INVETAQQ*** ***LQNQQDNR***GN IVKVNGPFGV
IRPPLRRGEG GQQPHEIA**NG** LEETLCTMRC TENLDDPSDA DVYKPSLGYI
STLNSYNLPI LRLLRLSALR GSIRKNAMVL PQWNVNANA LYVTNGKAHI
QMVNDNGERV FDQEISSGQL LVVPQGFSVM KHAIGEQFEW IEFK**TNENAQ**
VNTLAGRTSV MRG*LPLEVIT* NGYQISPEEA KRVKFSTIET TLTHSSPMSY
GRPRA

CRC

MVKLSNLLVA TFGVLLVLNG CLAR*QSLGVP PQLQNECNLD NLDVLQATET*
*IK****SEAGQIEY*** ***WDHNHPQLR***C VGVSVAR***YVI*** ***EQGGLYLPTF*** ***FTSPKISYVV***
QGTGISGR*VV PGCAETFMDS QPMQGQQQGQ PWQGR***QGQQG*** ***QPWEGQGQQG***
QQGRQGQPWE ***GQGQQGQQGR*** QGQQGQPWEG QGQQGQQGFR DMHQKVEHVR
RGDVFANTPG SAHWIYNSGE QPLVIIALLD IANYQNQLDR NPR***VFHLAGN***
NQQGGFGGSQ ***QQQEQKNLWS*** ***GFDAQVIAQA*** ***LKIDVQLAQQ*** ***LQNQQDSR***GN
IVRVKGPFQV VRPPLRQPYE SEEWRHPRSP QG**NG**LEETIC SMR**SHENIDD**
PARADVYKPS LGRVTSVNSY TLPILEYVRL SATRGVLQGN AMVLPKYNMN
ANEILYCTGG QGR**IQVVNDN** **GQNVLDQQVQ** K**GQ**LVVIPQG FAYVVQSHGN
K**FEWISFKTN** **ENAMISTLAG** R**TSLLRALPL** EVISNGFQIS PEEARKIK**FN**
TLETTLTRAA GRQQQQLIEE IVEA

CRU4

MARVSSLLSF CLTLLILFHG YAAQQGQQGQ QFPNECQLDQ LNALEPSHVL
KSEAGR***IEVW*** ***DHHAQLR***CSG VSFARYIIES K***GLYLPSFFN*** ***TAK***LSFVAKG
RGLMGK***VIPG*** ***CAETFQDSSE*** ***FQPR***FEGQGQ SQRFRDMHQK VEHIRSGDTI
ATTPGVAQWF YNDGQEPLVI VSVFDLASHQ NQLDRNPRPF YLAGNNPQGQ
VWLQGREQQP QKNIFNGFGP EVIAQALK***ID*** ***LQTAQQLQNQ*** ***DDNR***GNIVR***V***
QGPFGVIRPP ***LR***GQRPQEEE EEEGRHGRHG **NG**LEETICSA RCTDNLDDPS
R**ADVYKPQLG** **YISTLNSYDL** **PILR**FIRLSA LRGSIRQNAM VLPQWNANAN
AILYVTDGEA QIQIVNDNGN RVFDGQVSQG QLIAVPQGFS VVKRATSNR**F**
QWVEFKTNAN **AQINTLAGRT** SVLRGLPLEV ITNGFQISPE EARRVKFNTL
ETTLTHSSGP ASYGRPRVAA A

Fig. 4. Characterization of three accumulated proteins in *Atpme3-1*. (A) SDS-PAGE of total proteins (60 µg) extracted from 6-week-old WT and *Atpme3-1* plants. Gels were stained with Coomassie blue. (B) Western-blot and immuno-detection with an anti-cruciferin antibody. (C) Three gel bands in the *Atpme3-1* extracts (arrows in A) were further analysed by nano LC-MS/MS. The amino acids *NG* are boxed and indicate the cleavage site releasing the two subunits that comprise the CRUCIFERINS. The peptides analysed in the bands at 54 kDa are in bold, at 35 kDa in italic and at 21.5 kDa are underlined.

of its ubiquitous expression. Interestingly, comparison of electrophoretic profiles between WT and the A*tpme3-1* loss-of-function mutant showed significant differences (Fig. 1) suggesting that the knock-out mutation for *AtPME3* affects numerous processes in seedlings and adult plants.

Transcriptomic analysis was performed in *Atpme3-1 vs* WT hypocotyls to investigate the putative functions for AtPME3

Table 3. *Proteolytic activity of total, intracellular and cell wall protein extracts prepared from 6-week-old WT and Atpme3-1 Arabidopsis plants*

Activity was measured as described by Cupp-Enyard (2008) and expressed as nmol of tyrosine released min^{-1} mg of $proteins^{-1}$. Values are the mean±SD of four independent experiments. ANOVA, $^{*}P<0.05$ and $^{**}P<0.01$.

	Total proteins	Cellular proteins	Cell wall proteins
WT	10.2 ± 2.7	16.9 ± 4.1	8.8 ± 1.9
Atpme3-1	7.7 ± 1.6**	10.2 ± 2.3 *	5.1 ± 1.0 **

in early developmental stages of Arabidopsis (Fig. 2). Gene expression showed a dominant trend toward down-regulated expression of genes commonly expressed in roots and up-regulation of genes usually expressed in seeds. Thus, 16 down-regulated genes in hypocotyls belonged to the set of 24 genes which were previously described as being root hair specific (Won *et al.*, 2009). Three genes encoding expansins (*EXPA7*, *EXP17* and *EXP18*) are particularly interesting because they are involved in root hair initiation (Cho and Cosgrove, 2002). Accordingly, *Atpme3-1* seedlings showed an effective reduction in root hair number whereas their length was comparable to those from WT seedlings (Supplementary Fig. S2). As for adventitious rooting (Guénin *et al.*, 2011), PME3 might regulate the initiation of root hairs together with expansins in root epidermis. However, this regulation is not likely to occur at the transcriptomic level since none of the nine genes determining cell fate between hair and non-hair cells in root epidermis (Schiefelbein and Lee, 2006) were differentially expressed in *Atpme3-1*.

Most of the up-regulated genes in *Atpme3-1* hypocotyls encode proteins involved in seed development. Our data showed that germination of mutant seeds was faster than that of WT seeds (Fig. 5). In agreement, the expression of five genes encoding proteins specifically expressed during seed development were up-regulated. Previous results have shown that Arabidopsis seeds have high-level expression of *AtPME3* in micropylar endosperms and in radicles (Scheler *et al.*, 2015). Thus, AtPME3 could be more important for proper timing of germination than for cell wall remodeling during early seedling development, and longer hypocotyls in *Atpme3.1* could be due to earlier germination rather than to faster growth. This hypothesis is sustained by the same hypocotyl elongation rate measured from 4–5 days after germination (40 tested seedlings) in *Atpme3-1* (3.0 ± 0.5 mm) and in WT (3.2 ± 0.6 mm). Moreover, this presumed function for PME3 could work synergically with other proteins implicated in pectin metabolism that were also found to be down-regulated in our microarrays analysis, such as those encoding one PGase and four pectate lyases. These proteins and the three other AtPMEs could act as associated partners with AtPME3.

In wild type seedlings, two PME activity spots were detected by zymography in all seedling organs at pIs 9.2 and 9.6 except in cotyledons (Fig. 1). In *Atpme3-1*, the activity profile shows the expected absence of the spot at pI 9.6 that corresponds

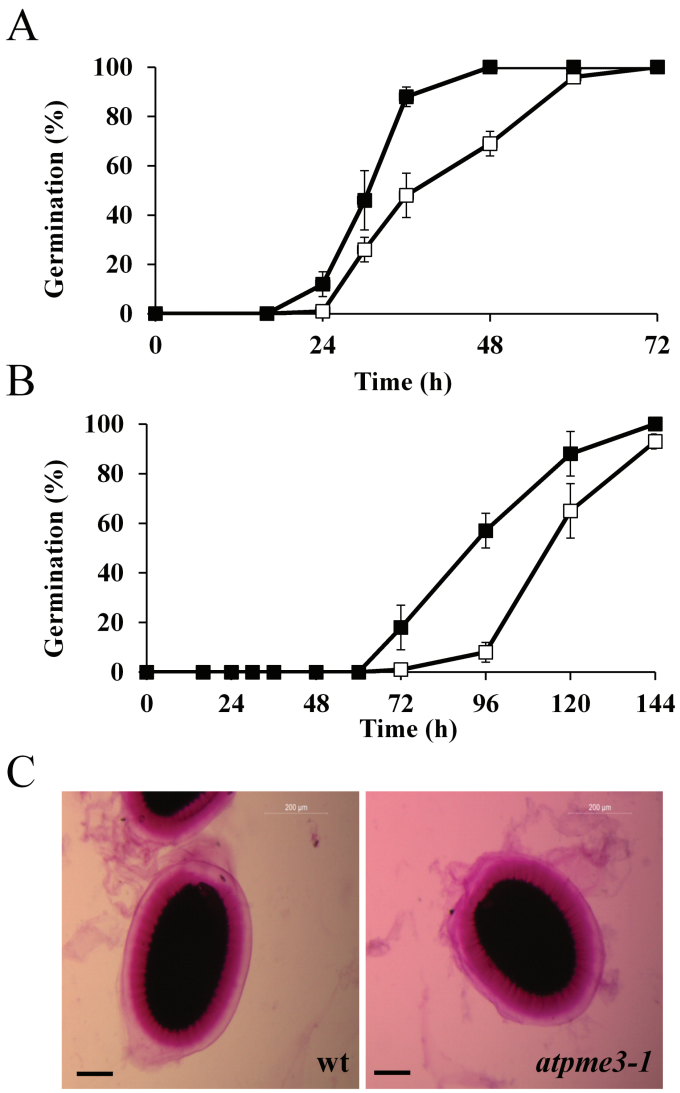

Fig. 5. Effect of ABA on the germination rate of *Atpme3-1* and the mucilage release during germination. (A, B) *In-vitro* germination rate of WT and *Atpme3-1* seeds on germination medium (A) or on germination medium supplemented with 1 µM ABA (B). Black squares represent *Atpme3-1* mutant and white squares represent WT. Means of four biological replicates±SD. (C) Staining of mucilage with ruthenium red after 3 h of imbibition. Scale bar: 1 mm. (This figure is available in colour at *JXB* online.)

to AtPME3 (Guénin *et al.*, 2011). Transcriptomic analysis shows that the loss of *AtPME3* expression is associated with a down-regulation of three other *PMEs*: *PME11*, *PME24* and *PME46*. These isoforms have theoretical pIs of about 5.78, 10.32 and 9.70. The decrease of this transcript abundance has no obvious effect on the PME activity levels on the zymogram. The only visible change is the disappearance of the activity spot at pI 9.6 in *Atpme3-1*, which is fully explained by *AtPME3* gene knock-out.

The normal development observed for *Atpme3-1* seedling implies the preservation of a sufficient PME activity level in the mutant hypocotyls, which could be related to a slower turnover of other PMEs. In agreement, five genes encoding proteases exhibited down-regulated expression, and a gene specifying a wall trypsin inhibitor-like protein was up-regulated in the mutant. In addition, seven out of 11 genes related to the ubiquitination pathway displayed a lower expression level in *Atpme3-1* leading to a possible reduction of protein degradation mediated by the 26S proteasome. Accordingly, proteolytic activity decreased by about 30–40% in *Atpme3-1* (Table 3). This reduction could maintain a steady state of PME activity. This PME activity preservation is probably noteworthy if one considers that ectopic expression of an AtPME inhibitor modifies phyllotaxy patterning in Arabidopsis plants (Peaucelle *et al.*, 2008). However, no report is currently available to our knowledge on a putative regulation performed by PME on proteolytic and proteasome activities. Moreover, inhibition of these activities in *Lepidium sativum* seeds provoked a decrease or cessation of endosperm weakening necessary for germination, contrasting with our results where mutant seeds germinated earlier (Morris *et al.*, 2011).

Another molecular trait particularly visible in *Atpme3-1* seedlings and 6-week-old plants was the accumulation of a 21.5-kDa protein (Fig. 1), with two other bands at 54 and 35 kDa that were more visible in adult plants (Fig. 4). Polypeptides of these molecular masses are in agreement with reported values for unprocessed CRUCIFERINS and their α- and β-subunits (Li *et al.*, 2007; Wan *et al.*, 2007).

Western blot analysis using anti-cruciferin antibodies revealed two bands at 54 and 35 kDa that were clearly detected in *Atpme3-1* but only faintly in WT (Fig. 4). The protein band at 21.5 kDa was not recognized by the antibodies, which is not surprising since CRUCIFERIN β-subunit is poorly antigenic with these antibodies (Wan *et al.*, 2007). Nano LC-MS/MS analyses confirmed that CRUCIFERINS were effectively present in mutant hypocotyls and plants. From the two bands recognized by the antibodies and from the band at 21.5 kDa, analyses have identified peptides sequenced from CRB, CRC and CRU4 CRUCIFERINS. Moreover, genes encoding these three CRUCIFERINS were overexpressed in the mutant (Fig. 3). In addition, while CRD/At1g03890 was not detected by nano LC-MS/MS analyses, the gene exhibits an up-regulated expression both in microarray and in RT-qPCR data. However, this CRUCIFERIN is poorly represented in WT Arabidopsis seeds (Wan *et al.*, 2007).

CRUCIFERIN subunit proteolysis generally starts with the α-chain via its C-terminal extremity during seed germination and is followed by complete β-chain degradation during radicle emergence (Li *et al.*, 2007). Normally, unprocessed CRUCIFERINS and their subunits would be reduced to trace levels in seedlings. However, a possible slowdown of protein degradation may explain these differences in accumulated CRUCIFERIN amounts in the mutant. The apparent link between cell wall-localized AtPME3 and CRUCIFERINS in vacuoles is unclear and further studies are required to increase our understanding of the sustained mechanism.

Phenotypic traits characterizing the *AtPME3* loss-of-function included faster germination of seeds (Fig. 5) and a reduced root-hair density of seedlings (Supplementary Fig. S2). In 4-day-old etiolated hypocotyls from *Atpme3-1*, expression is disrupted for a large set of genes, among

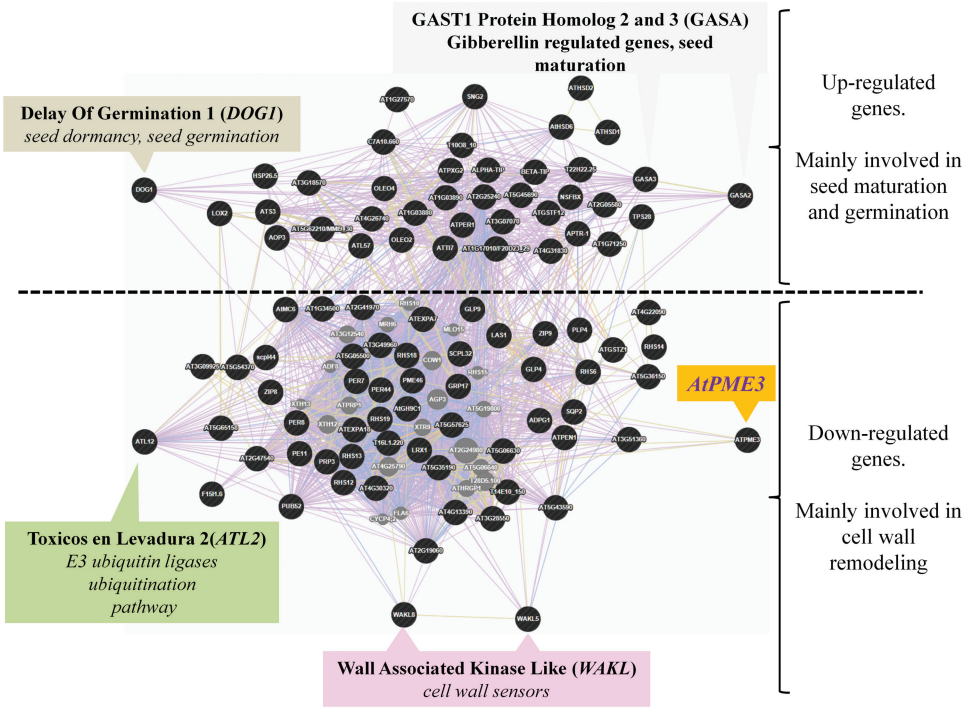

Fig. 6. Network of co-expression built with regulated genes listed from the transcriptomic data in the *Atpme3-1* mutant compared with WT. This network was built with GeneMANIA (Warde-Farley *et al.*, 2010) by using *AtPME3* and 95 genes listed from the microarray analysis. The full list of genes and their names are in Table S6. Two groups of co-expressed genes clearly appeared: the one shown in the upper part of the figure is devoted to storage functions and the one in the bottom part to cell wall remodeling. Up-regulated genes (DOG1, GASA2 and GASA3) or down-regulated genes (ATL2, WAKL5 and WAKL8) are highlighted. (This figure is available in colour at *JXB* online.)

which GA-related genes and two *WAKL* genes are down-regulated. *WAKL* genes, encoding receptor-like kinases, are known for their essential role in cell expansion during plant growth (Verica and He, 2002). These proteins are considered to play a role as wall sensors strongly bound to pectins by their extracellular moiety (Verica *et al.*, 2003; Steinwand and Kieber, 2010). AtPME3 action on pectins and signal transduction via WAKL5 and/or WAKL8 could interact, with intracellular consequences. Recently, the existence of an interaction between WAK2, another receptor kinase, and AtPME3 was suggested (Kohorn *et al.*, 2014). Demethylation of pectins by AtPME3 might control binding of WAK2's extracellular domain with polymers and could be implicated in signal transduction upon stress. Another receptor-like kinase, present in the expression network built around AtPME3, is required to maintain cell wall integrity and to allow root hair growth (Boisson-Dernier *et al.*, 2015). Molecular targets for such receptor kinases in Arabidopsis remain unknown (De Smet *et al.*, 2009); however, our results suggest that these wall sensors may have some impact on reservoir activity of triacylglycerols and CRUCIFERINS and, possibly, on protein turnover. Further clarification of the role of AtPME3 in reserve mobilization is fundamental as this process has significant consequences in subsequent seedling growth stages.

Supplementary data

Supplementary data are available at *JXB* online.

Fig. S1. RT-qPCR analyses of the expression of four *CRUCIFERIN* genes in *Atpme3-1* dry seeds and in 1-, 2- and 4-day-old seedlings grown in the dark.

Fig. S2. Phenotypic characterization of roots of 4-day-old WT and *Atpme3-1* seedlings grown in the dark.

Table S1. List of genes implicated in plant development that are differentially expressed in 4-day-old hypocotyls of WT and *Atpme3-1* seedlings.

Table S2. List of genes implicated in cell wall (except pectin) metabolism that are differentially expressed in 4-day-old hypocotyls of WT and *Atpme3-1* seedlings.

Table S3. List of genes implicated in lipid metabolism and associated to storage functions that are differentially expressed in 4-day-old hypocotyls of WT and *Atpme3-1* seedlings.

Table S4. List of genes implicated in protein metabolism that are differentially expressed in 4-day-old hypocotyls of WT and *Atpme3-1* seedlings.

Table S5. Sequence coverage of CRUCIFERINS (%) identified by nano LS-MS/MS in WT and *Atpme3-1* plants.

Table S6. List of genes used in the co-expression network and presented in Fig. 6.

Acknowledgements

The authors are grateful to Mrs Anne Gée for her excellent technical assistance as well as to the Université de Rouen Normandie and the Université de Picardie Jules Verne for their constant logistic help. We thank Dr D. Hegedus (Canada) for the gift of antibodies directed against cruciferins, and Dr A. Voxeur (INRA Versailles) for helpful discussions. Cell imaging facility (PRIMACEN) and proteomic platform (PISSARO) (Université de Rouen

Normandie), research network GRR Végétal-Agronomie-Sol-Innovation (VASI)-Région Haute Normandie (France) and the Regional Council of Picardie—Hauts de France are also acknowledged. Part of work was supported by ANR (ANR-09-BLANC-0007-01 Projet GROWPEC).

References

Abramoff MD, Magalhaes PJ, Ram SJ. 2004. Image processing with ImageJ. Biophotonics International **11,** 36–42.

Bertheau Y, Madgidi-Hervan E, Kotoujansky A, Nguyen-The C, Andro T, Coleno A. 1984. Detection of depolymerase isoenzymes after electrophoresis or electrofocusing, or in titration curves. Analytical Biochemistry **139,** 383–389.

Bewley JD, Black M. 1994. Seeds: physiology of development and germination. New York: Plenum Press.

Boisson-Dernier A, Franck CM, Lituiev DS, Grossniklaus U. 2015. Receptor-like cytoplasmic kinase MARIS functions downstream of CrRLK1L-dependent signaling during tip growth. Proceedings of the National Academy of Sciences, USA **112,** 12211–12216.

Bove J, Jullien M, Grappin P. 2001. Functional genomics in the study of seed germination. Genome Biology **3,** reviews1002.

Bradford MM. 1976. A rapid and sensitive method for the quantitation of microgram quantities of protein utilizing the principle of protein-dye binding. Analytical Biochemistry **72,** 248–254.

Carpita NC, Gibeaut DM. 1993. Structural models of primary cell walls in flowering plants: consistency of molecular structure with the physical properties of the walls during growth. The Plant Journal **3,** 1–30.

Cho HT, Cosgrove DJ. 2002. Regulation of root hair initiation and expansin gene expression in Arabidopsis. The Plant Cell **14,** 3237–3253.

Cupp-Enyard C. 2008. Sigma's non-specific protease activity assay—casein as a substrate. Journal of Visualized Experiments, e899.

Derbyshire P, McCann MC, Roberts K. 2007. Restricted cell elongation in Arabidopsis hypocotyls is associated with a reduced average pectin esterification level. BMC Plant Biology **7,** 31.

De Smet I, Voss U, Jürgens G, Beeckman T. 2009. Receptor-like kinases shape the plant. Nature Cell Biology **11,** 1166–1173.

Fait A, Angelovici R, Less H, Ohad I, Urbanczyk-Wochniak E, Fernie AR, Galili G. 2006. Arabidopsis seed development and germination is associated with temporally distinct metabolic switches. Plant Physiology **142,** 839–854.

Gallardo K, Job C, Groot SP, Puype M, Demol H, Vandekerckhove J, Job D. 2001. Proteomic analysis of arabidopsis seed germination and priming. Plant Physiology **126,** 835–848.

Gallardo K, Job C, Groot SP, Puype M, Demol H, Vandekerckhove J, Job D. 2002. Importance of methionine biosynthesis for Arabidopsis seed germination and seedling growth. Physiologia Plantarum **116,** 238–247.

Gendreau E, Traas J, Desnos T, Grandjean O, Caboche M, Höfte H. 1997. Cellular basis of hypocotyl growth in *Arabidopsis thaliana*. Plant Physiology **114,** 295–305.

Goldberg R, Morvan C, Roland JC. 1986. Composition, properties and localization of pectins in young and mature cells of the mung bean hypocotyl. Plant & Cell Physiology **27,** 417–429.

Gruis D, Schulze J, Jung R. 2004. Storage protein accumulation in the absence of the vacuolar processing enzyme family of cysteine proteases. The Plant Cell **16,** 270–290.

Guénin S, Mareck A, Rayon C, *et al*. 2011. Identification of pectin methylesterase 3 as a basic pectin methylesterase isoform involved in adventitious rooting in *Arabidopsis thaliana*. The New Phytologist **192,** 114–126.

Gutierrez L, Conejero G, Castelain M, Guénin S, Verdeil JL, Thomasset B, Van Wuytswinkel O. 2006. Identification of new gene expression regulators specifically expressed during plant seed maturation. Journal of Experimental Botany **57,** 1919–1932.

Gutierrez L, Mauriat M, Guénin S, *et al*. 2008. The lack of a systematic validation of reference genes: a serious pitfall undervalued in reverse transcription-polymerase chain reaction (RT-PCR) analysis in plants. Plant Biotechnology Journal **6,** 609–618.

Ham BK, Li G, Kang BH, Zeng F, Lucas WJ. 2012. Overexpression of Arabidopsis plasmodesmata germin-like proteins disrupts root growth and development. The Plant Cell **24,** 3630–3648.

Hewezi T, Howe P, Maier TR, Hussey RS, Mitchum MG, Davis EL, Baum TJ. 2008. Cellulose binding protein from the parasitic nematode *Heterodera schachtii* interacts with *Arabidopsis pectin* methylesterase: cooperative cell wall modification during parasitism. The Plant Cell **20,** 3080–3093.

Holdsworth MJ, Bentsink L, Soppe WJ. 2008. Molecular networks regulating Arabidopsis seed maturation, after-ripening, dormancy and germination. The New Phytologist **179,** 33–54.

Horton P, Park KJ, Obayashi T, Fujita N, Harada H, Adams-Collier CJ, Nakai K. 2007. WoLF PSORT: protein localization predictor. Nucleic Acids Research **35,** W585–W587.

Irshad M, Canut H, Borderies G, Pont-Lezica R, Jamet E. 2008. A new picture of cell wall protein dynamics in elongating cells of *Arabidopsis thaliana*: confirmed actors and newcomers. BMC Plant Biology **8,** 94.

Jolie RP, Duvetter T, Van Loey AM, Hendrickx ME. 2010. Pectin methylesterase and its proteinaceous inhibitor: a review. Carbohydrate Research **345,** 2583–2595.

Klavons JA, Bennett AD. 1986. Determination of methanol using alcohol oxidase and its application to methyl ester content of pectins. Journal of Agricultural and Food Chemistry **34,** 597–599.

Kohorn BD, Kohorn SL, Saba NJ, Martinez VM. 2014. Requirement for pectin methyl esterase and preference for fragmented over native pectins for wall-associated kinase-activated, EDS1/PAD4-dependent stress response in Arabidopsis. The Journal of Biological Chemistry **289,** 18978–18986.

Kucera B, Cohn MA, Leubner-Metzger G. 2005. Plant hormone interactions during seed dormancy release and germination. Seed Science Research **15,** 281–307.

Laemmli UK. 1970. Cleavage of structural proteins during the assembly of the head of bacteriophage T4. Nature **227,** 680–685.

Li Q, Wang BC, Xu Y, Zhu YX. 2007. Systematic studies of 12S seed storage protein accumulation and degradation patterns during Arabidopsis seed maturation and early seedling germination stages. Journal of Biochemistry and Molecular Biology **40,** 373–381.

Linkies A, Müller K, Morris K, *et al*. 2009. Ethylene interacts with abscisic acid to regulate endosperm rupture during germination; a comparative approach using *Lepidium sativum* (cress) and *Arabidopsis thaliana*. The Plant Cell **21,** 3803–3822.

Mäser P, Thomine S, Schroeder JI, *et al*. 2001. Phylogenetic relationships within cation transporter families of Arabidopsis. Plant Physiology **126,** 1646–1667.

Morris K, Linkies A, Müller K, Oracz K, Wang X, Lynn JR, Leubner-Metzger G, Finch-Savage WE. 2011. Regulation of seed germination in the close Arabidopsis relative *Lepidium sativum*: a global tissue-specific transcript analysis. Plant Physiology **155,** 1851–1870.

Ouidir T, Jarnier F, Cosette P, Jouenne T, Hardouin J. 2015. Characterization of N-terminal protein modifications in *Pseudomonas aeruginosa* PA14. Journal of Proteomics **114,** 214–225.

Peaucelle A, Louvet R, Johansen JN, Höfte H, Laufs P, Pelloux J, Mouille G. 2008. Arabidopsis phyllotaxis is controlled by the methyl-esterification status of cell-wall pectins. Current Biology **18,** 1943–1948.

Pelletier S, Van Orden J, Wolf S, *et al*. 2010. A role for pectin de-methylesterification in a developmentally regulated growth acceleration in dark-grown Arabidopsis hypocotyls. The New Phytologist **188,** 726–739.

Refrégier G, Pelletier S, Jaillard D, Höfte H. 2004. Interaction between wall deposition and cell elongation in dark-grown hypocotyl cells in Arabidopsis. Plant Physiology **135,** 959–968.

Ren C, Kermode AR. 2000. An increase in pectin methyl esterase activity accompanies dormancy breakage and germination of yellow cedar seeds. Plant Physiology **124,** 231–242.

Scheler C, Weitbrecht K, Pearce SP, *et al*. 2015. Promotion of testa rupture during garden cress germination involves seed compartment-specific expression and activity of pectin methylesterases. Plant Physiology **167,** 200–215.

Schiefelbein J, Lee MM. 2006. A novel regulatory circuit specifies cell fate in the *Arabidopsis* root epidermis. Physiologia Plantarum **26,** 503–510.

Sénéchal F, Wattier C, Rustérucci C, Pelloux J. 2014. Homogalacturonan-modifying enzymes: structure, expression, and roles in plants. Journal of Experimental Botany **65,** 5125–5160.

Sénéchal F, L'Enfant M, Domon JM, *et al*. 2015. Tuning of pectin methylesterification: pectin methylesterase inhibitor 7 modulates the processive activity of co-expressed pectin methylesterase 3 in a pH-dependent manner. The Journal of Biological Chemistry **290,** 23320–23335.

Shevchenko A, Wilm M, Vorm O, Mann M. 1996. Mass spectrometric sequencing of proteins silver-stained polyacrylamide gels. Analytical Chemistry **68,** 850–858.

Shimada T, Yamada K, Kataoka M, *et al*. 2003. Vacuolar processing enzymes are essential for proper processing of seed storage proteins in *Arabidopsis thaliana*. The Journal of Biological Chemistry **278,** 32292–32299.

Simon A, Biot E. 2010. ANAIS: analysis of NimbleGen arrays interface. Bioinformatics **26,** 2468–2469.

Steinwand BJ, Kieber JJ. 2010. The role of receptor-like kinases in regulating cell wall function. Plant Physiology **153,** 479–484.

Towbin H, Staehelin T, Gordon J. 1979. Electrophoretic transfer of proteins from polyacrylamide gels to nitrocellulose sheets: procedure and some applications. Proceedings of the National Academy of Sciences, USA **76,** 4350–4354.

Vandesompele J, De Preter K, Pattyn F, Poppe B, Van Roy N, De Paepe A, Speleman F. 2002. Accurate normalization of real-time quantitative RT-PCR data by geometric averaging of multiple internal control genes. Genome Biology **3**, research0034.1.

Verica JA, Chae L, Tong H, Ingmire P, He ZH. 2003. Tissue-specific and developmentally regulated expression of a cluster of tandemly arrayed cell wall-associated kinase-like kinase genes in Arabidopsis. Plant Physiology **133,** 1732–1746.

Verica JA, He ZH. 2002. The cell wall-associated kinase (WAK) and WAK-like kinase gene family. Plant Physiology **129,** 455–459.

Verwoerd TC, Dekker BMM, Hoekema A. 1989. A small-scale procedure for the rapid isolation of plant RNAs. Nucleic Acids Research **17,** 2362.

Wan L, Ross AR, Yang J, Hegedus DD, Kermode AR. 2007. Phosphorylation of the 12 S globulin cruciferin in wild-type and abi1-1 mutant *Arabidopsis thaliana* (thale cress) seeds. The Biochemical Journal **404,** 247–256.

Warde-Farley D, Donaldson SL, Comes O, *et al*. 2010. The GeneMANIA prediction server: biological network integration for gene prioritization and predicting gene function. Nucleic Acids Research **38,** W214–W220.

Weber M, Deinlein U, Fischer S, Rogowski M, Geimer S, Tenhaken R, Clemens S. 2013. A mutation in the *Arabidopsis thaliana* cell wall biosynthesis gene pectin methylesterase 3 as well as its aberrant expression cause hypersensitivity specifically to Zn. The Plant Journal **76,** 151–164.

Western TL, Burn J, Tan WL, Skinner DJ, Martin-McCaffrey L, Moffatt BA, Haughn GW. 2001. Isolation and characterization of mutants defective in seed coat mucilage secretory cell development in Arabidopsis. Plant Physiology **127,** 998–1011.

Willats WG, Orfila C, Limberg G, *et al*. 2001. Modulation of the degree and pattern of methyl-esterification of pectic homogalacturonan in plant cell walls. Implications for pectin methyl esterase action, matrix properties, and cell adhesion. The Journal of Biological Chemistry **276,** 19404–19413.

Wolf S, Hématy K, Höfte H. 2012. Growth control and cell wall signaling in plants. Annual Review of Plant Biology **63,** 381–407.

Wolf S, Mouille G, Pelloux J. 2009. Homogalacturonan methyl-esterification and plant development. Molecular Plant **2,** 851–860.

Won SK, Lee YJ, Lee HY, Heo YK, Cho M, Cho HT. 2009. Cis-element- and transcriptome-based screening of root hair-specific genes and their functional characterization in Arabidopsis. Plant Physiology **150,** 1459–1473.

Zhao C, Craig JC, Petzold HE, Dickerman AW, Beers EP. 2005. The xylem and phloem transcriptomes from secondary tissues of the Arabidopsis root-hypocotyl. Plant Physiology **138,** 803–818.